Numerical Heat Transfer, Part A, 44: 183–197, 2003

ISSN: 1040-7782 print/1521-0634 online
DOI: 10.1080/10407780390206634

Taylor & Francis
Taylor & Francis Group

DISCRETE TRANSFER METHOD APPLIED TO TRANSIENT RADIATIVE TRANSFER PROBLEMS IN PARTICIPATING MEDIUM

P. Rath
Department of Mechanical Engineering, Indian Institute of Technology, North Guwahati, Assam, India

S. C. Mishra
Institute of Fluid Mechanics (LSTM), University of Erlangen-Nuremberg, Erlangen, Germany

P. Mahanta and U. K. Saha
Department of Mechanical Engineering, Indiana Institute of Technology, North Guwahati, Assam, India

K. Mitra
Department of Mechanical & Aerospace Engineering, Florida Institute of Technology, Melbourne, Florida, USA

Application of the discrete transfer method is extended to solve transient radiative transport problems with participating medium. A one-dimensional gray planar absorbing and anisotropically scattering medium is considered. Both boundaries of the medium are black. The incident boundary of the medium is subjected to pulse-laser irradiation, while the other boundary is cold. For radiative parameters such as optical thickness, scattering albedo, anisotropy factor, transmittance, and reflectance at the boundaries are found. Results obtained from the present work are compared with those available in the literature. The discrete transfer method has been found to give an excellent agreement.

INTRODUCTION

Thermal radiation is important in many applications, and its analysis is difficult in the presence of a participating medium. Thermal radiation being electromagnetic waves, it propagates at the speed of light. In most traditional engineering applications, such as in the thermal analysis of boilers, furnaces, internal combustion engines, etc., as temporal variations in thermal quantities of interest are much slower than the time scale associated with the propagation of thermal radiation, the

Received 21 May 2002; accepted 2 December 2002.
Address correspondence to Prof. Subhash C. Mishra, Department of Mechanical Engineering, Indian Institute of Technology (IIT), Guwahati, North Guwahati, Guwahati 781039, Assam, India. E-mail: scm_iitg@yahoo.com

NOMENCLATURE

c	speed of light, m/s	μ'	incoming direction of propagation
I	intensity, W/m^2	σ_s	scattering coefficient, m^{-1}
L	physical depth of the medium, m	τ	optical thickness
n	number of control volumes	ϕ	azimuthal angle, rad
p	phase function	ω	scattering albedo
Q	heat flux, W/m^2		
S	source function, W/m^2	**Subscripts**	
t	time, s	c	collimated
x	space coordinate, m	d	diffuse
β	extinction coefficient, m^{-1}	0	incident direction of collimated beam
θ	polar angle, rad		
μ	$\cos\theta$	**Superscripts**	
μ_0	incident cosine angle of the collimated beam	*	for nondimensional time

transient term from the radiative transfer equation is neglected, i.e., radiation is assumed to be an instantaneous (steady-state) process. However, there are certain situations in which temporal variations are required at time scales as low as 10^{-12} to 10^{-15} s. Therefore, such situations necessitate inclusion of the transient term in the radiative transfer equation, thus making problems further complicated.

Some examples in which the transient nature of thermal radiation has to be considered are microscale systems [1], pulsed-laser interactions with materials [2, 3], laser-induced shock waves [4], laser therapy [5–7], optical tomography [8, 9], remote sensing of turbid media of oceans and the atmosphere [10, 11], probing of the characteristics of the particulate medium by examining the transmitted or back-scattered intensities [12], and particle detection and sizing [13]. A detailed review dealing with various aspects of transient radiative transport has been given by Kumar and Mitra [14].

In the literature, applications of various existing methods used for solving steady-state radiative transport problems have been extended for the analysis of transient radiative transport in a participating medium. Rackmil and Buckius [15] used the finite-difference method with an adding-doubling scheme to solve the transient equation of transfer for a plane-parallel slab. Diffusion approximation has been used by Flock et al. [16] and Yamada [8]. As is true with the solution of steady-state radiative transport problems, diffusion approximation has been found to give correct predictions only for optically thick conditions. For low to thin optical thickness conditions, it has not been found suitable [17]. Kumar et al. [18] and Mitra et al. [19] have extended the use of the P-1 approximation to the solution of transient radiative transport for 1-D and 2-D rectangular geometries. Mitra and Churnside [11] have applied the discrete ordinates method for the solution of a transient radiative equation applied to oceanographic lidar. The Monte Carlo method has been used by Guo et al. [20, 21] and Schweiger et al. [22]. Tan and Hsu [23] have used a time-dependent integral formulation for modeling transient radiative transfer, and application of the radiation element method for this class of problems has been extended by Guo and Kumar [24].

A comparative study of the two-flux method, P-1 approximation, and the discrete ordinates method has been presented by Mitra and Kumar [25]. They compared the parabolic as well as hyperbolic nature of short-pulse radiative transport. They found that for higher optical thickness, both hyperbolic and parabolic solutions become identical. Further, they found that the wave propagation speed depends on the method used. With P-1 approximation and the two-flux method, the propagation speed of wave front has been found to be far away from the speed of the pulse. This lower propagation speed could have the potential drawback of predicting results that have a significant temporal mismatch with the observed data. But such discrepancy is low with the discrete ordinates method. However, the discrete ordinates method is prone to ray and false scattering effects, and it is severe in multidimensional geometry. Hence, the scope for further study remains open to other numerical methods.

The discrete transfer method (DTM) [26] is one of the popular methods for solving radiative transfer problems. It combines good features of the zonal method, the flux method, and the Monte Carlo method. For steady-state problems in various types of geometries, this method has been used extensively for pure radiation as well as radiation, conduction, and/or convection heat transfer problems. However, for the analysis of transient radiative heat transfer problems, applicability of this method has not been explored so far. The present work thus aims at extending the use of the DTM for a new class of problems.

In the present work, the effect of a short-pulse laser at one boundary of a planar medium is investigated using the DTM. The other boundary is diffuse and is at zero temperature. The cold medium is assumed to be absorbing and anisotropically scattering. Temporal variations of transmissivity and reflectivity at the medium boundaries are computed for different optical thicknesses, scattering albedos, and anisotropy factors. Results from the present study are compared with those from [27]. Very good agreement has been found between the two.

FORMULATION

Consider a plane-parallel absorbing and anisotropically scattering gray medium (Figure 1). The top boundary is irradiated with a short-pulse laser beam of magnitude $I(\mu_0, \phi)$ at an angle (μ_0, ϕ). The bottom boundary is cold. Both the boundaries are assumed black. For azimuthally symmetric radiation $[I(\mu, \phi) = I(\mu)]$, which is always the case for radiative transport in a planar medium, the radiative transfer equation (RTE) in any direction μ is written as

$$\frac{1}{c}\frac{\partial I(x,\mu,t)}{\partial t} + \mu\frac{\partial I(x,\mu,t)}{\partial x} = -\beta I(x,\mu,t) + \frac{\sigma_s}{2}\int_{-1}^{1} I(x,\mu',t)p(\mu',\mu)d\mu' \qquad (1)$$

where c is the speed of light, β is the extinction coefficient, σ_s is the scattering coefficient, and $p(\mu', \mu)$ is the phase function. For the problem under consideration, the intensity at the top boundary is given by

$$I(\mu, t) = I(\mu_0, t)\delta(\mu - \mu_0) \qquad (2)$$

where δ is the Dirac delta function. Since the top boundary is subjected to the collimated laser beam, radiation inside the medium is composed of collimated I_c as

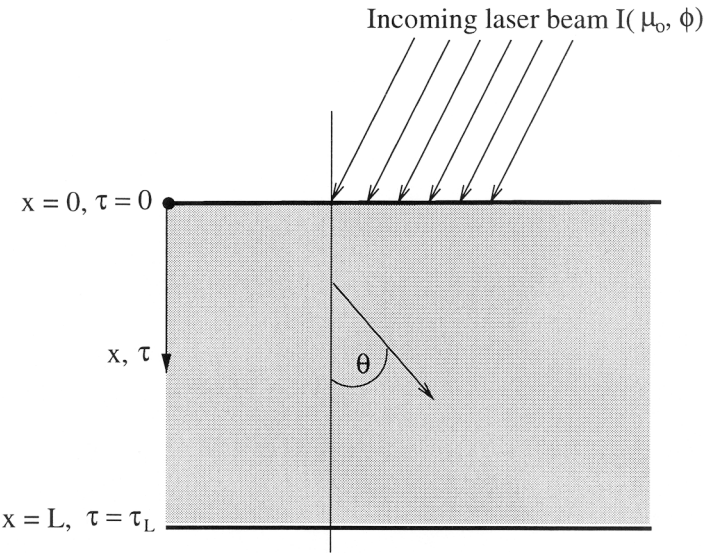

Figure 1. One-dimensional planar geometry under consideration.

well as the diffuse I_d components, i.e., radiation at any physical depth x in any direction μ at any instant t can be written as

$$I(x, \mu, t) = I_c(x, \mu, t) + I_d(x, \mu, t) \tag{3}$$

Substitution of Eq. (3) into Eq. (1) results in

$$\frac{\partial I_d(\tau, \mu, t^*)}{\partial t^*} + \mu \frac{\partial I_d(\tau, \mu, t^*)}{\partial \tau} + I_d(x, \mu, t^*) = \frac{\omega}{2} \int_{-1}^{1} I_d(\tau, \mu', t^*) p(\mu', \mu) d\mu' + S_c(x, \mu, t^*) \tag{4}$$

where $t^* = \beta c t$, $\tau = \beta x$, and ω is the scattering albedo. In the above equation, the out-scattered radiation source S_C formed because of the collimated irradiation is given by

$$S_c(\tau, \mu, t^*) = \frac{\omega}{4\pi} \int_0^{2\pi} \int_{-1}^{1} p(\mu', \mu) I_c(\tau, \mu', t^*) d\mu' d\phi \tag{5}$$

where $I_c(\tau, \mu, t^*)$ is obtained by solving the RTE governing the attenuation of the collimated beam and is given by

$$I_c(\tau, \mu, t^*) = I(\mu_0, t^*) \exp\left(-\frac{\tau}{\mu_0}\right) \times \left[H\left(t^* - \frac{\tau}{\mu_0}\right) - H\left(t^* - t_p^* - \frac{\tau}{\mu_0}\right)\right] \delta(\mu - \mu_0) \delta(\phi - \phi_0) \tag{6}$$

where H is the Heaviside step function and t_p^* is nondimensional pulse width.

In Eq. (5), if anisotropy is approximated by a linear anisotropic phase function $[p(\mu', \mu) = 1 + a\mu\mu']$, the collimated source function for the south bound ($0 \leqslant \mu < 1$) and the north bound ($-1 \leqslant \mu \leqslant 0$) intensities are given respectively by

$$S_c^S(\tau, \mu, t^*) = \frac{\omega}{4\pi}\epsilon_N I(\mu_0, t^*)(1 + a\mu\mu_0) \times \exp\left(-\frac{\tau}{\mu_0}\right)\left[H\left(t^* - \frac{\tau}{\mu_0}\right) - H\left(t^* - t_p^* - \frac{\tau}{\mu_0}\right)\right] \tag{7}$$

and

$$S_c^N(\tau, \mu, t^*) = \frac{\omega}{4\pi}\epsilon_N I(\mu_0, t^*)(1 - a\mu\mu_0) \times \exp\left(-\frac{\tau}{\mu_0}\right)\left[H\left(t^* - \frac{\tau}{\mu_0}\right) - H\left(t^* - t_p^* - \frac{\tau}{\mu_0}\right)\right] \tag{8}$$

In the above equations, a is the anisotropy factor and its value ranges from $+1$ to -1. For $a > 0$, scattering is forward; whereas for $a < 0$, it is backward. For $a = 0$, it is isotropic scattering, and in this case, for intensities in all directions, expressions of S_C are the same and are given by

$$S_c(\tau, \mu, t^*) = \frac{\omega}{4\pi} I(\mu_0, t^*) \exp\left(-\frac{\tau}{\mu_0}\right)\left[H\left(t^* - \frac{\tau}{\mu_0}\right) - H\left(t^* - t_p^* - \frac{\tau}{\mu_0}\right)\right] \tag{9}$$

Equation (4) is the required integro-differential equation to be solved. To make the solution of the governing equation feasible by the DTM, the first term on the left-hand side of this equation is written in finite-difference form using the backward Euler scheme. This results in the following equation:

$$\frac{I_d(\tau, \mu, t^*) - I_d(\tau, \mu, t^* - \Delta t^*)}{\Delta t^*} + \mu\frac{\partial I_d(\tau, \mu, t^*)}{\partial \tau} + I_d(\tau, \mu, t) = \frac{\omega}{2}\int_{-1}^{1} I_d(\tau, \mu', t^*)p(\mu', \mu)d\mu' + S_c(\tau, \mu, t^*) \tag{10}$$

Rearranging the terms in the above equation gives

$$A\mu\frac{dI_d(\tau, \mu, t^*)}{d\tau} + I_d(\tau, \mu, t^*) = AS_c(\tau, \mu, t^*) + AS_d(\tau, \mu, t^*) + \frac{I_d(\tau, \mu, t^* - \Delta t^*)}{1 + \Delta t^*} \tag{11}$$

where $A = \frac{\Delta t^*}{(1+\Delta t^*)}$ and the source function

$$S_d(\tau, \mu, t^*) = (1 - \omega)I_b(\tau, t^*) + \frac{\omega}{4\pi}[G(\tau, t^*) + a\mu q_{\text{net}}(\tau, t^*)] \tag{12}$$

In Eq. (12), G and q_{net} are incident radiation and net heat flux, respectively, and this form of Eq. (12) results from approximating the anisotropy by linear anisotropic phase function. In the DTM, G and q_{net} are computed from

$$G(\tau, t^*) = 2\pi \int_{\theta=0}^{\pi} I(\tau, \mu, t^*) \sin\theta \, d\theta = 2\pi \sum_{i=0}^{m} I(\tau, \mu_i, t^*) \sin\theta_i \sin(\Delta\theta) \tag{13}$$

$$\begin{aligned} q_{\text{net}}(\tau, t^*) &= 2\pi \int_{\theta=0}^{\pi} I(\tau, \mu, t^*) \sin\theta \cos\theta \, d\theta \\ &= 2\pi \sum_{i=0}^{m} I(\tau, \mu_i, t^*) \sin\theta_i \cos\theta_i \sin(\Delta\theta) \end{aligned} \tag{14}$$

where m is the total numbers of intensities considered over the spherical polar angle for the numerical integration.

To facilitate evaluation of Eqs. (13) and (14), for any direction μ at a given time t^*, Eq. (11) is integrated between upstream point τ_n and downstream point τ_{n+1} in the following way:

$$\begin{aligned} &\int_{\tau_n}^{\tau+1} d\left[\exp\left(\frac{\tau}{\mu}\right) I_d(\tau, \mu, t^*)\right] \\ &= \frac{A}{A\mu} \int_{\tau_n}^{\tau_{n+1}} S_c(\tau, \mu, t^*) \exp\left(\frac{\tau}{A\mu}\right) d\tau + \frac{A}{A\mu} \int_{\tau_n}^{\tau_{n+1}} S_c(\tau, \mu, t^*) \exp\left(\frac{\tau}{A\mu}\right) d\tau \\ &\quad + \frac{1}{(1+\Delta t^*) A\mu} \int_{\tau_n}^{\tau_{n+1}} I_d(\tau, \mu, t^* - \Delta t^*) \exp\left(\frac{\tau}{A\mu}\right) d\tau \end{aligned} \tag{15}$$

If the optical path leg between the upstream and the downstream points in a given intensity direction μ is small enough, the source terms S_C, S_d, and I_d appearing inside the integrals on the right-hand side of Eq. (13) can be assumed constant and equal to the average of their values at the two points. Under this condition, Eq. (15) results in

$$\begin{aligned} I_d(\tau_{n+1}, \mu, t^*) &= I_d(\tau_n, \mu, t^*) \exp\left(-\frac{\Delta\tau}{A\mu}\right) + AS_c^{\text{av}} \left[1 - \exp\left(-\frac{\Delta\tau}{A\mu}\right)\right] \\ &\quad + AS_d^{\text{av}} \left[1 - \exp\left(-\frac{\Delta\tau}{A\mu}\right)\right] + \frac{I_d^{\text{av}}}{1+\Delta t^*} \left[1 - \exp\left(-\frac{\Delta\tau}{A\mu}\right)\right] \end{aligned} \tag{16}$$

where

$$\begin{aligned} S_c^{\text{av}} = \frac{\omega}{8\pi} I(\mu_0, t^*) \Bigg\{ &\exp\left(-\frac{\tau_{n+1}}{\mu_0}\right) \left[H\left(t^* - \frac{\tau_{n+1}}{\mu_0}\right) - H\left(t^* - t_p^* - \frac{\tau_{n+1}}{\mu_0}\right)\right] \\ &+ \exp\left(-\frac{\tau_n}{\mu_0}\right) \left[H\left(t^* - \frac{\tau_n}{\mu_0}\right) - H\left(t^* - t_p^* - \frac{\tau_n}{\mu_0}\right)\right] \Bigg\} \end{aligned} \tag{17}$$

$$S_d^{\text{av}} = \frac{1}{2} [S_d(\tau_{n+1}, \mu, t^*) + S_d(\tau_n, \mu, t^*)] \tag{18}$$

$$I_d^{\text{av}} = \frac{1}{2} [I_d(\tau_{n+1}, \mu, t^* - \Delta t^*) + I_d(\tau_n, \mu, t^* - \Delta t^*)] \tag{19}$$

With the recursive use of Eq. (16), at any time level t^*, intensity distributions at all the desired points are computed. In the expression for S_d [Eq. (12)], the values of G and q_{net} are computed using Eqs. (13) and (14).

In transient radiative transport problems, transmittance and reflectance are the main radiative quantities of interest. Transmittance is defined as net radiative heat flux emerging out of the medium due to transmission, and in the problem under consideration it is the net radiative heat flux $Q^+(t^*, \tau_L)$ at the bottom boundary ($\tau = \tau_L$). Reflectance is the net radiative heat flux from the boundary which is subjected to laser irradiation, and in the present case it is the reflected heat flux $Q^-(t^*, 0)$ at the top boundary ($\tau = 0$). For evaluation of these quantities, integration over polar angle θ in Eqs. (13) and (14) is performed over 0 to $\pi/2$.

RESULTS AND DISCUSSION

In the following sections, results of the time-varying nondimensional transmissivity and reflectivity obtained from the DTM are presented for various values of optical thickness τ_L, scattering albedo ω, and anisotropy factor a. For pulse-laser irradiation normal to the top boundary ($\mu_0 = 1$), all these results are presented for the nondimensional pulse width $\beta c t_p = 1$. For calculation of transmissivity and reflectivity, intensity has been nondimensionalized by dividing it by the intensity of the collimated laser beam I_O. For some cases, DTM results are compared with the results obtained by the piecewise parabolic advection (PPA) scheme along with the discrete ordinates method [27].

As the DTM is a ray-tracing method, and in the numerical scheme the solution domain is divided into a finite number of control volumes, accuracy of the DTM results depends on the number of rays, number of control volumes, and in the present case of a transient problem, the time step used. In the present work, for various sets of radiative parameters, for rays, spatial grid-and temporal grid-independent situations, numerical experiments were performed, and beyond 45 rays, 500 control volumes, and a time step of $\Delta t^* = 0.001$, results have not been found to change. However, for lower values of τ_L and ω, for rays and grid-independent situation, fewer rays and control volumes are required. In the present work, all results have been presented for rays and grid-independent situation.

In Figures 2 and 3, effects of optical thickness τ_L on time-varying transmittance and reflectance are shown, respectively. For $\tau_L = 1$, 5, and 10, these results are presented for isotropic scattering ($a = 0$) with $\omega = 0.998$.

It is seen from Figures 2*a*–2*c* that with increase in τ_L, not only the peak value of the transmittance decreases, but also its decay rate decreases. In other words, for lower values of τ_L, transmittance signal remains available only for a shorter duration. It is seen from Figures 3*a*–3*c* that the peak value of the reflectance is the same for all values of τ_L, but the decay rates are different, and like the transmittance signal, for higher τ_L, it takes longer time to die out.

In transient radiation analysis, radiation takes some finite time to travel the optical depth of the medium. The greater the optical depth of the medium, the more time is taken by the radiation to travel from one boundary to the other. Because of this fact, as observed in Figures. 2*a*–2*c*, transmittance signals are found available

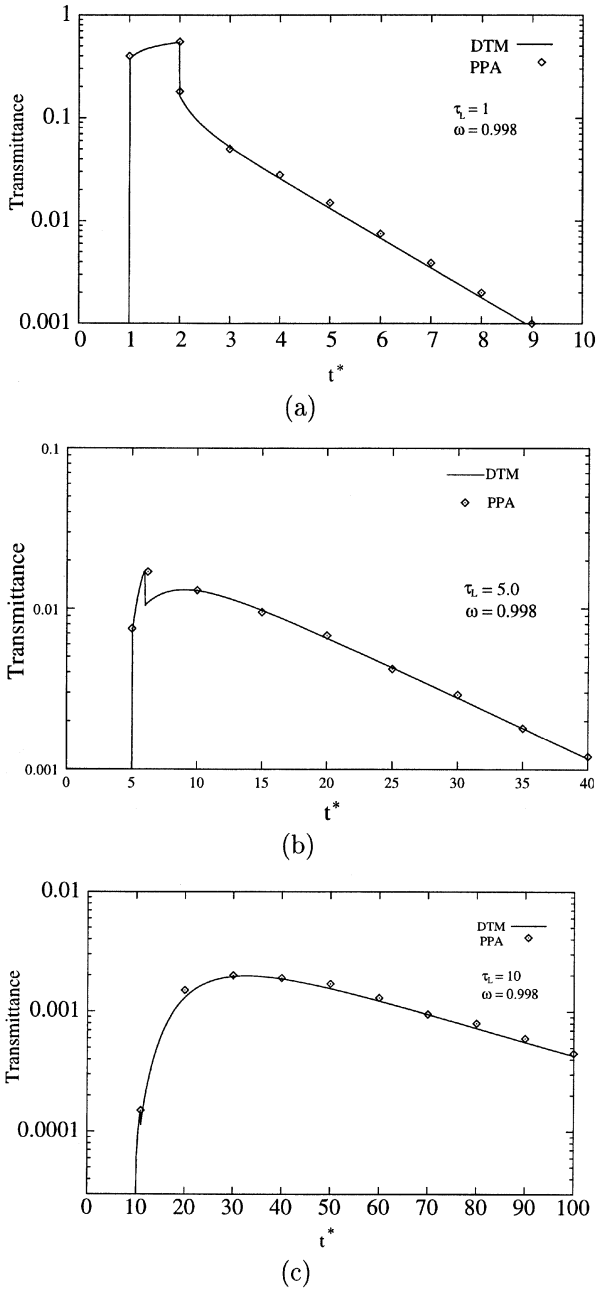

Figure 2. Effects of optical thickness τ_L on time-varying transmittance $[Q^+(t^*, \tau_L)]$; $a = 0$, $\omega = 0.998$.

only after the time radiation has reached the other (bottom) boundary, and this time is different for different optical thicknesses. However, as seen from Figures 3*a*–3*c*, the reflectance signal is available as soon as the boundary is subjected to the pulse-laser source.

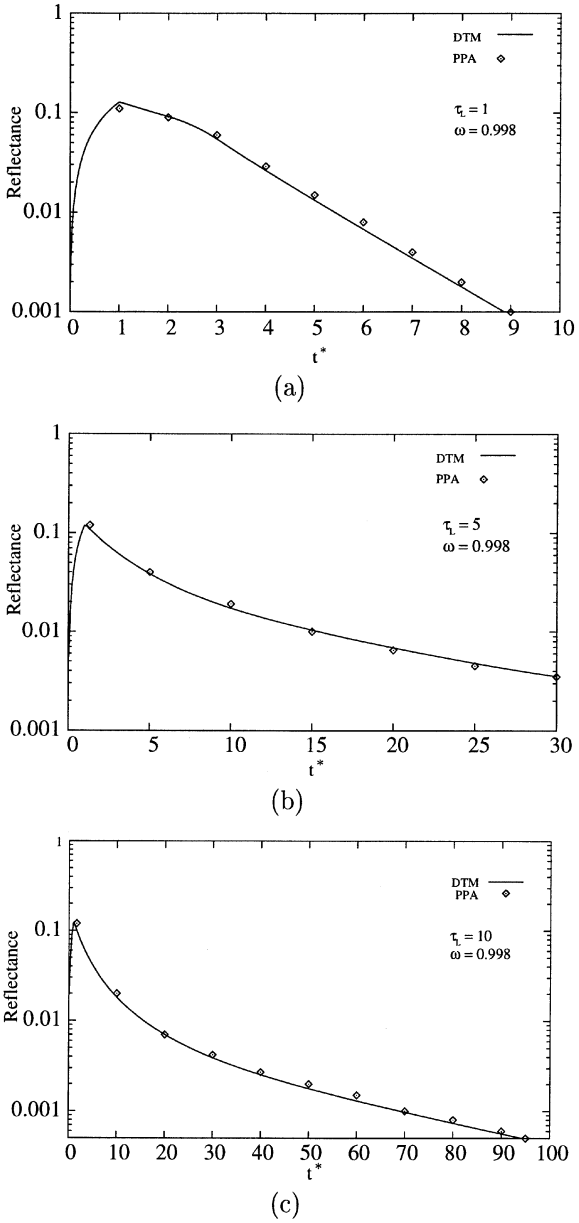

Figure 3. Effects of optical thickness τ_L on time-varying reflectance $[Q^-(t^*, 0)]$; $a = 0$, $\omega = 0.998$.

For all the cases above, DTM results have been compared with the piecewise parabolic advection (PPA) scheme along with the discrete ordinates method [27]. Results from both methods compare well.

In Figures 4 and 5, effects of scattering albedo ω on transmittance and reflectance respectively, are shown. For $a = 0$, these results are shown for $\tau_L = 1$, 5,

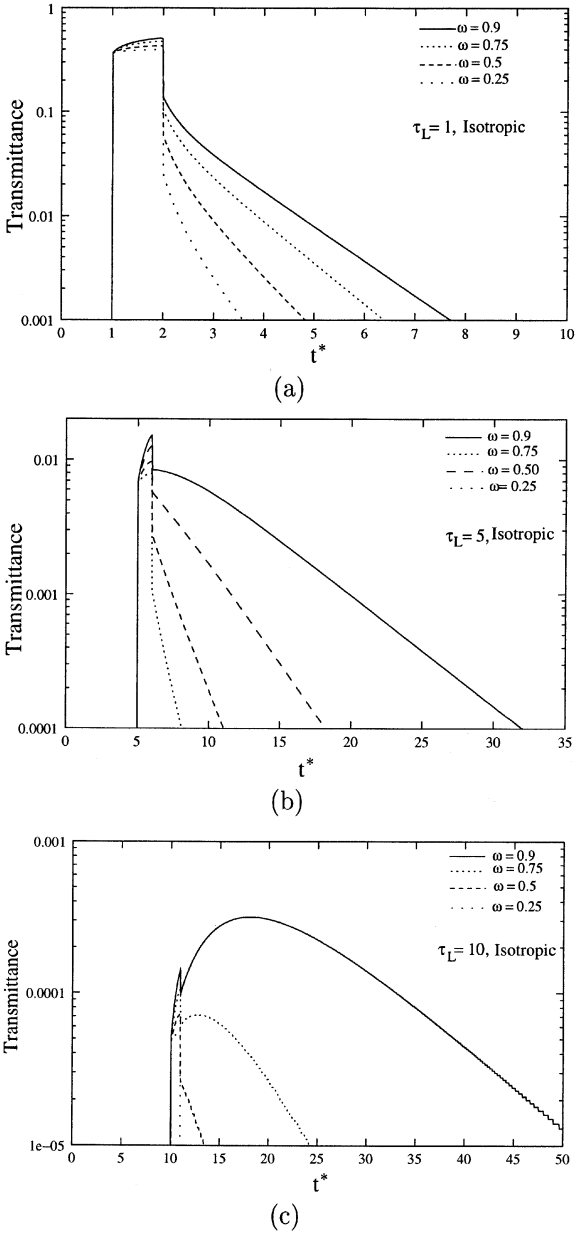

Figure 4. Effects of scattering albedo ω on time-varying transmittance $[Q^+(t^*, \tau_L)]$ for (*a*) optical thickness $\tau_L = 1$, (*b*) $\tau_L = 5$, and (*c*) $\tau_L = 10$.

and 10. It is seen from Figures 4*a*–4*c* that for any τ_L, the effect of ω is very strong, and this effect is more pronounced for higher values of τ_L. For lower values of τ_L, the peak value of the transmittance is higher, and for different ω, they do not differ much. As time passes, this difference grows. For all τ_L values, it is observed that for

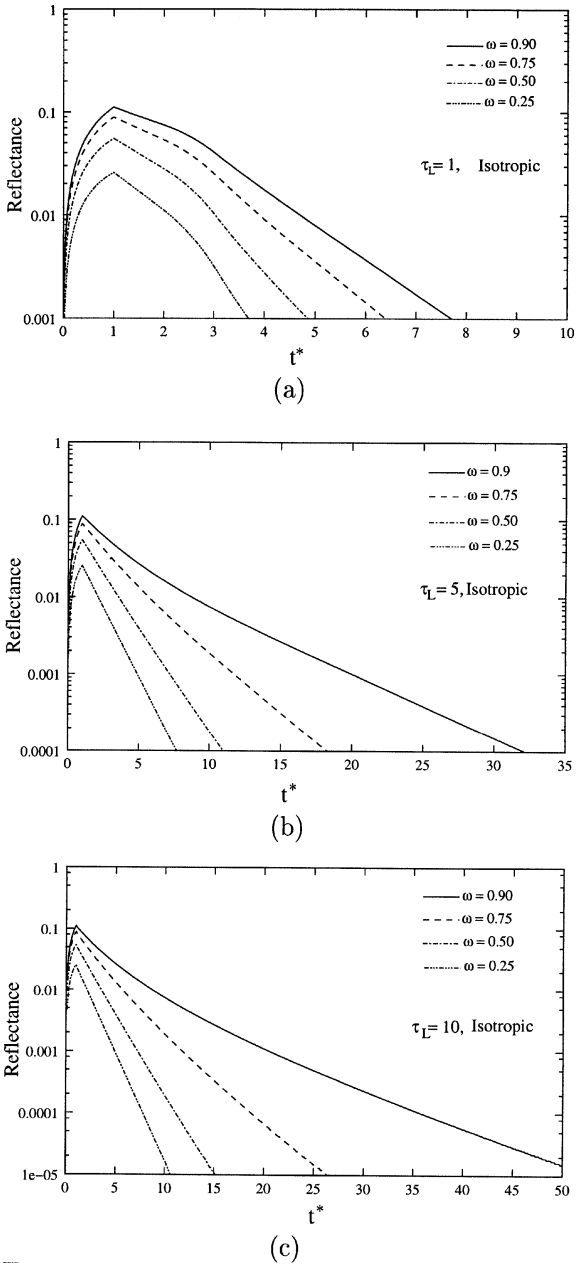

Figure 5. Effects of scattering albedo ω on time-varying reflectance $[Q^{-}(t^{*},0)]$ for (*a*) optical thickness $\tau_L = 1$, (*b*) $\tau_L = 5$, and (*c*) $\tau_L = 10$.

higher values of ω, the transmittance signal remains available for longer duration, and this duration increases for higher τ_L values. However, this availability decreases with decrease in ω values. For a given τ_L, the above trend is due to the fact that the

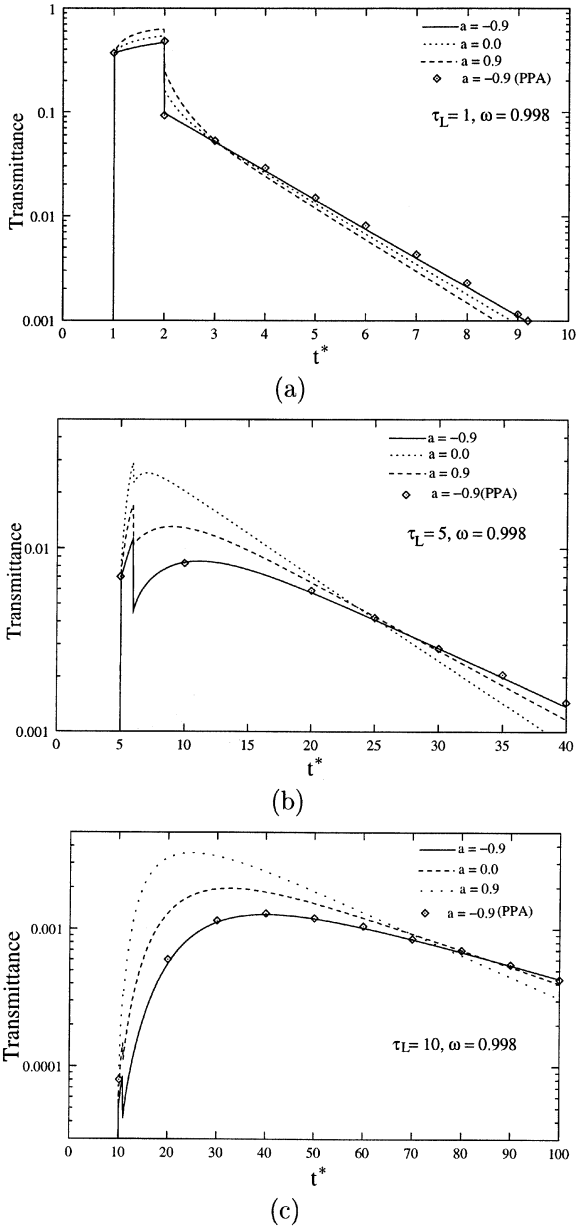

Figure 6. Effects of anisotropy a on transmittance $[Q^+(t^*, \tau_L)]$ for (a) $\tau_L = 1$, (b) $\tau_L = 5$, and (c) $\tau_L = 10$; $\omega = 0.998$.

higher the value of ω, the higher is the scattering phenomenon, and hence radiation suffers multiple scattering before emerging out of the medium.

Trends similar to these for the effects of ω on transmittance are also observed for reflectance calculations (Figures 5*a*–5*c*). For all τ_L, the peak values decrease with decrease in ω. Availability of the reflectance signal also decreases with decrease in ω.

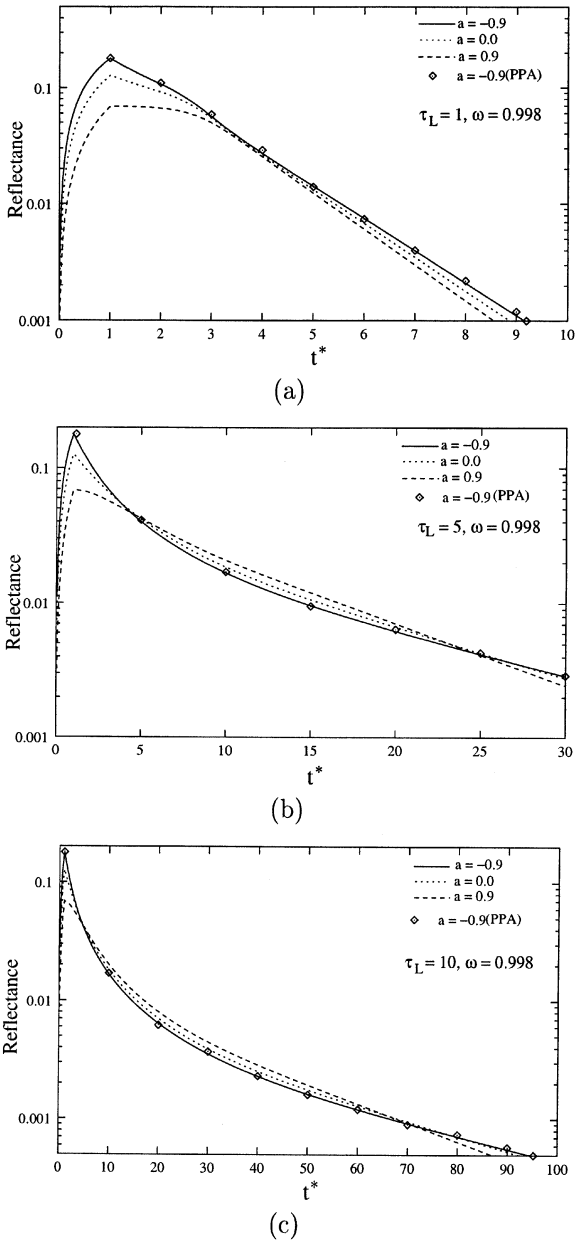

Figure 7. Effects of anisotropy a on reflectance $[Q^{-}(t^{*},0)]$ for (a) $\tau_L = 1$, (b) $\tau_L = 5$, and (c) $\tau_L = 10$; $\omega = 0.998$.

Effects of anisotropy factor a on transmittance and reflectance are shown in Figures 6 and 7, respectively. For $\omega = 0.998$, effects of anisotropy are shown for $\tau_L = 1$, 5, and 10. Two values of anisotropy factor ($a = +0.9$ and $a = -0.9$) close to the extreme limits of forward scattering ($a = +1$) and backward scattering ($a = -1$) are chosen. Results for isotropic scattering ($a = 0$) are also given.

It is seen from Figures. 6*a*–6*c* that the peak values of transmittance are higher for the forward scattering ($a > 0$) than for the backward scattering ($a < 0$). The difference in the peak values increases with increase in τ_L. Further, the signal decay rate is also less for the backward scattering. A reduced decay rate for backward scattering is because of the fact that in this case, as compared to the forward and isotropic scattering situations, radiation tends to stay in the medium for longer duration.

As far as effect of a on decay rate of reflectance signal is concerned (Figures 7*a*–7*c*), it is similar to its effects on transmittance. But unlike its effect on transmittance, the effect is less pronounced for higher values of τ_L. In both Figures 6 and 7, for $a = -9$, DTM results are compared with those from the PPA [27]. Both methods are found to compare very well.

CONCLUSIONS

Application of the discrete transfer method has been extended, for the first time, to solve transient radiative transport problems in a participating medium. The formulation presented has been validated by solving transient radiative transfer problems in a one-dimensional planar absorbing and scattering medium, one boundary of which is subjected to a short-pulse laser and the other boundary of which is cold. Effects of optical thickness, scattering albedo, and anisotropy factor on transmittance and reflectance have been studied. For some sample cases, results have been compared with those available in the literature. The discrete transfer method has been found to work well for the transient radiative transport problems.

REFERENCES

1. A. Majumdar, Microscale Energy Transport in Solids, in C. L. Tien (ed.), *Microscale Energy Transport*, pp. 1–93. Beggel House, New York, 1998.
2. J. P. Longtin and C. L Tien, Saturable Absorption during High Intensity Laser Heating of Liquids, *J. of Heat Transfer*, vol. 118, pp. 924–930, 1996.
3. H. K. Park, D. Kim, C. P. Grigoropoulos, and A. C. Tam, Pressure Generation and Measurement in the Rapid Vaporization of Water on Pulsed Laser Heated Source, *J. Appl. Phys.*, vol. 80, no. 7, pp. 4072–4083, 1996.
4. J. Noack and A. Vogel, Single-Shot Spatially Resolved Characterization of Laser Induced Shock Waves in Water, *Appl. Opt.*, vol. 37, no. 19, pp. 4092–4099, 1998.
5. M. J. C. Gemert and J. J. Wetch, Clinical Use of Laser-Tissue Interaction, *JEEE Eng. Med. Biol. Mag.*, pp. 100–113, 1989.
6. D. P. Poppas, G. B. Rucker, and D. S. Scerr, Laser Tissue Welding—Poised for the New Millenium, *Surg. Technol. Int.,* vol. 9, pp. 33–41, 2000.
7. H. G. Pettit and R. Sauerbrey, Pulsed Ultraviolet Laser Ablation, *Appl. Phys. A*, vol. 56, pp. 51–63, 1993.
8. Y. Yamada, *Light-Tissue Interaction and Optical Imaging in Biomedicine*, vol. 6, PP. 1–59, Begell House, New York, 1995.
9. F. Liu, K. M. Yoo, and R. R. Alfano, Ultra-fast Laser Pulse Transmission and Imaging through Biological Tissues, *Appl. Opt.,* vol. 32, no. 4, pp. 554–558, 1993.
10. R. E. Walker and J. W. Mclean, Lidar Equations for Turbid Media with Pulse Stretching, *Appl. Opt.*, vol. 38, pp. 2384–2397, 1999.
11. K. Mitra and J. H. Churnside, Transient Radiative Transfer Equation Applied to Oceanographic Lidar, *Appl. Opt.*, vol. 38, no. 6, pp. 889–895, 1999.

12. S. A. Prahl, M. J. C. Van Gemert, and A. J. Welch, Determining the Optical Properties of Turbid Media by using the Adding-Doubling Method, *Appl. Opt.*, vol. 32, pp. 559–568, 1993.
13. K. J. Grant, J. A. Piper, D. J. Ramsay, and K. L. Williams, Pulse Lasers in Particle Detection and Sizing, *Appl. Opt.*, vol. 32, pp. 416–417, 1993.
14. S. Kumar and K. Mitra, Microscale Aspects of Thermal Radiation Transport and Laser Applications, *Adv. Heat Transfer*, vol. 33, pp. 187–294, 1999.
15. C. I. Rackmil and R. O. Buckius, Numerical Solution Technique for the Transient Equation of Transfer, *Numer. Heat Transfer*, vol. 6, pp.135–153, 1983.
16. S. T. Flock, M. S. Patterson, B. C. Wilson, and D. R. Wyman, Monte Carlo Modelling of Light Propagation in Highly Scattering Tissues—I: Prediction and Comparison of Diffusion Theory, *IEEE Trans. Biomed. Eng.*, vol. 36, pp. 1162–1168, 1989.
17. K. M. Yoo, F. Liu, and R. R. Alfano, When Does the Diffusion Approximation Fail to Describe Photon Transport in Random Media, *Phys. Rev. Lett.*, vol. 64, pp. 2647–2650, 1990.
18. S. Kumar, K. Mitra, and Y. Yamada, Hyperbolic Damped-Wave Models for Transient Light-Pulse Propagation in Scattering Media, *Appl. Opt.*, vol. 35, no. 19, pp. 3372–3378, 1996.
19. K. Mitra, M. S. Lai, and S. Kumar, Transient Radiation Transport in Participating Media within a Rectangular Enclosure, *J. Thermophys. Heat Transfer*, vol. 11, no. 3, pp. 409–414, 1997.
20. Z. Guo, S. Kumar, and K. C. San, Multi-dimensional Monte Carlo Simulatiion of Short-Pulse Laser Transport in Scattering Media, *J. Quant. Spectros. Radiat.*, vol. 14, no. 4, 504–511, 2000.
21. Z. Guo, B. A. Garetz J. Aber, and S. Kumar, Monte Carlo Simulation and Experiments of Pulsed Radiative Transfer, *J. Quant. Spectros. Radiat. Transfer*, vol. 73, pp. 159–168, 2002.
22. H. Schweiger, A. Oliva, M. Costa, and C. D. P. Segarra, A Monte Carlo Method for the Simulation of Transient Radiation Heat Transfer: Application to Compound Honeycomb Transparent Insulation, *Numer. Heat Transfer B*, vol. 35, no. 1, pp. 113–136, 2001.
23. Z. M. Tan and P. F. Hsu, An Integral Formulation of Transient Radiative Transfer, *Journal of Heat Transfer*, vol. 123, pp. 466–475, 2001.
24. Z. Guo and S. Kumar, Radiation Element Method for Transient Hyperbolic Radiative Transfer in Plane-Parallel Inhomogeneous Media, *Numer. Heat Transfer B*, vol. 39, no. 4, pp. 371–387, 2001.
25. K. Mitra and S. Kumar, Development and comparison of models for light-pulse transport through scattering-absorbing media, *Applied Optics*, vol. 38, no. 1, 188–196, 1999.
26. N. G. Shah, New method of Computation of Radiant Heat Transfer in Combustion Chambers. Ph.D. thesis, Imperial College, University of London, England, 1979.
27. M. Sakami, K. Mitra, and P. F. Hsu, Transient Radiative Transfer in Anisotropically Scattering Media Using Monotonicity-Preserving Schemes, 2000 Int. Mechanical Engineering Congress and Exposition, November 5–10, 2000, Orlando, FL, USA.